Journal of Molecular Graphics and Modelling 46 (2013) 52–58

Contents lists available at ScienceDirect

Journal of Molecular Graphics and Modelling

journal homepage: www.elsevier.com/locate/JMGM

Conformational preference of glycinamide in solution: An answer derived from combined experimental and computational studies

Bishwajit Ganguly[a,*], Manoj K. Kesharwani[a], Nikola Basarić[b], Eringathodi Suresh[a], Abul Kalam Biswas[a], Kata Mlinarić-Majerski[b,*]

[a] Analytical Discipline and Centralized Instrument Facility, Central Salt & Marine Chemicals Research Institute (Council of Scientific and Industrial Research) Bhavnagar, Gujarat 364 002, India
[b] Department of Organic Chemistry and Biochemistry, Ruđer Bošković Institute, Bijenička cesta 54, P.O. Box 180, 10 002 Zagreb, Croatia

ARTICLE INFO

Article history:
Accepted 11 September 2013
Available online 20 September 2013

Keywords:
Glycinamide
Solvent effect
NMR
DFT
Conformer stability

ABSTRACT

Conformational problems are often subtle but very important in controlling many intricate features in chemistry and biochemistry. We have performed the conformational analysis of glycinamide using NMR experiments and computational studies. ^{1}H NMR experiments suggest the prevalence of intramolecular hydrogen bonded conformation of glycinamide (**2B**) in acetonitrile, whereas, non-intramolecular hydrogen bonded conformation **2A** is favoured in dimethylsulfoxide. The NOESY experiments carried out for glycinamide in DMSO-d_6, showed stronger NOE interaction of the N**H$_a$**-atom of amide group with C**H$_2$** than that of N**H$_b$**-atom confirming the presence of conformer **2A**. DFT calculations performed with explicit DMSO molecules also suggested a clear preference for the conformer **2A**. The molecular dynamics simulations performed with the explicit DMSO molecules also showed that the intermolecular hydrogen bonding exists between the solvent and solute molecules to stabilize the conformer **2A**. The present study sheds light on the debate of conformational preference of neutral glycinamide in the present literature.

1. Introduction

The amide functional groups are of considerable interest to researchers due to their presence from chemistry to biochemistry. This is a fundamental linkage in building blocks of biomolecules, *i.e.* protein and other kinds of bioactive molecules [1,2]. Naturally occurring polypeptide chains, found in proteins, are heteropolymers of α-amino acid residues linked together by peptide bonds and are dependent on the conformational preference of the amide groups [1,2]. Glycinamide is a simple derivative of glycine and is the simplest amide, which is important to form complexes and an appropriate model compound for *N*-terminal amino acids in peptides.

Besides its importance in peptides and proteins, glycinamide has also been used to examine the habit of rock salt [3]. The computational results revealed the relative significance of conformations of glycinamide towards the morphology of salt crystals [3]. Two stable conformers of glycinamide discussed in the literature are given in Scheme 1 [4,5].

Sulzbach et al. have performed the quantum chemical study to examine the conformational behaviour of glycinamide. The *ab initio* quantum chemical calculations revealed that the glycinamide conformer with torsional angle $\psi_{(4,3,2,1)} = 165^\circ$ (**2A**) is a global minimum and 1.3 kcal/mol lower than conformer that has $\psi_{(4,3,2,1)} = 2^\circ$ (**2B**) (Scheme 1) [4]. The structural assignments of **2A** and **2B** were carried out with the NMR calculations. Structures of peptides in solution are obtained by two- and three-dimensional Fourier-transform (FT) NMR experiments [6]. Recently, Bu and co-workers have performed extensive study towards understanding the conformational behaviour of glycinamide using density functional theory in both the gas and aqueous phases [5]. The B3LYP/6-311++G** calculated results suggested that the glycinamide conformer **2B** is energetically preferred than **2A** in both the mediums. They have found similar results with single point energy calculations at higher-level computations, including the MP2, MP3, MP4SDQ, and CCSD(T) methods employing the aug-cc-pVDZ basis set. The calculations performed by Bu et al. confronted the earlier predictions of conformational preference of glycinamide [4]. However, it has been observed that in the aqueous phase the energy difference between the two conformers is smaller than the gas phase calculated results [5].

The influence of glycinamide conformers on the crystal morphology of NaCl crystals was apparent in the aqueous phase calculations [3]. The experimental observations suggest that glycinamide is not a habit modifier for sodium chloride crystals. The inability of glycinamide as a habit modifier of rock-salt is envisaged due to the predominant presence of conformer **2A** in the aqueous

* Corresponding authors. Fax: +91 278 2567562.
E-mail addresses: ganguly@csmcri.org (B. Ganguly), majerski@irb.hr (K. Mlinarić-Majerski).

1093-3263/$ – see front matter © 2013 Elsevier Inc. All rights reserved.
http://dx.doi.org/10.1016/j.jmgm.2013.09.007

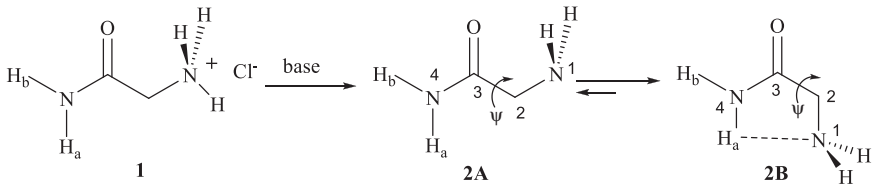

Scheme 1. Glycinamide hydrochloride (**1**) and two stable conformers (**2A** and **2B**) of glycinamide.

medium [3]. It is also known that the solution behaviour comprises a much greater challenge in the conformational analysis at the molecular level [7,8]. Therefore, these results prompted us to re-examine the conformational behaviour of glycinamide in solvent, which, however, is a subject of debate in the literature.

The hydrogen bonding between the solute and the solvent molecules can control the relative stability of the conformers. Such interactions alter the conformational equilibria dramatically in polar solvents [7–10]. The influence of hydrogen bonding of polar solvent molecules with the solutes is not considered in the continuum solvation model calculations. Glycinamide has polar functional groups which can participate in hydrogen bonding with the polar solvent molecules. Therefore, it is important to examine the influence of hydrogen bonding of solvent molecules on the stability of glycinamide conformers. The calculations with single explicit water molecule have been reported [11], in which the water molecule is interacting with only the amide oxygen, but it lacks the interaction of solvent molecule with the polar hydrogens of glycinamide. In the present study, we have examined the influence of solvent molecules on the conformational behaviour of glycinamide with extensive NMR study in DMSO-d_6 and CD_3CN followed by molecular dynamics study using the same solvent molecules. The solvent DMSO is known to form hydrogen bonds, whereas, CD_3CN will participate less in such interactions with the substrate molecules [12–14].

2. Methodology

2.1. Experimental details

2.1.1. Methods

^1H and 2D NOESY spectra were recorded on a Bruker Spectrometer at 300 or 600 MHz. NMR spectra were measured in DMSO-d_6, CD_3CN or C_6D_6 using tetramethylsilane as a reference. The mixing time used in the NOESY experiments for glycinamide hydrochloride (**1**) and glycinamide (**2**) in DMSO was 0.3 s. The mixing time in the NOESY experiments for glycinamide (**2**) in CH_3CN was 0.1, 0.3, 0.5, and 0.9 s.

2.1.2. Materials

Glycinamide hydrochloride (**1**) is commercially available, whereas glycinamide (**2**) was prepared by deprotonation of **1**. In a flask (50 mL) was placed glycinamide hydrochloride (**1**, 80 mg, 0.72 mmol), K_2CO_3 (2 g, 145 mmol) and anhydrous CH_3CN (50 mL). The slurry was stirred over 4 h at rt. Insoluble salts were filtered off, and from the remaining solution solvent was removed on a rotary evaporator to afford glycinamide (30 mg, 56%).

2.2. Computational details

The two-dimensional potential energy surfaces were constructed by varying the O—C—C—N and C—C—N—H torsional angle for rotation of 180° with increments of 10° in both gas phase and solvent medium using Becke3 Lee Yang Parr functional and 6-311++G** basis set [15–17]. The default polarizable continuum solvation model (PCM) was employed for the solvent calculations [18–22]. The default UFF radii were used for the PCM calculations, which incorporate explicit hydrogen atoms. The desired conformers were further optimized with same method in respective solvation medium. A hybrid approach of explicit and implicit continuum model was also used to optimize both conformers of glycinamide (**2A** and **2B**) with six molecules of solvent (DMSO). Single point calculations were performed at MP2/6-311++G** level using B3LYP optimized geometries. Two dimensional potential energy scan were performed using Gaussian 03 program, whereas, all other calculations were performed using Gaussian 09 program [23,24].

The molecular dynamic simulations were performed using density functional theory method employing DMol^3 suit program. The LDA/PWC/DND methods were employed for dynamics calculations [25–27]. The simulation cell was a periodically repeated cubic box of side length 15 Å. The conductor-like screening solvation model (COSMO) was employed to incorporate the continuum dielectric constant environment for DMSO (ε = 46.7) [18,28]. The whole simulations were performed with the canonical NVT ensemble and temperature is controlled at 25 °C and 80 °C with the Nosé–Hoover chain thermostat. In each case, initially the simulations were performed for 1 ps with a time step of 2 fs. For the case of conformer **2A**, simulations were further extended up to 2 ps. The statistics were collected every 2 fs for all simulations.

3. Results and discussion

Initially, extensive computational search was performed to examine the influence of dielectric constant of dimethylsulfoxide (DMSO) and acetonitrile on the relative stabilities of glycinamide conformers. The conformational changes associated with the rotation of C—C bond and C—$N_{(amine)}$ bond were analyzed by constructing a two-dimensional potential energy scan using B3LYP/6-311++G** method [15–17] in both the gas phase and implicit solvent mediums (DMSO and acetonitrile) (Fig. 1 and Fig. S1, Supporting information). To construct the potential energy surface representing the effect of the internal rotation—the C—C and C—$N_{(amine)}$ bonds were allowed to rotate 180° with increments of 10° in all the studied mediums. The lowest energy forms of **2A** and **2B** were chosen from potential energy surfaces in each medium and further optimized without any constraint using B3LYP/6-311++G** methods in the respective medium. Additionally, highest energy conformers were chosen from potential energy surfaces and further considered for transition state optimizations at the same level of theory in each studied medium. Single point calculations were performed to compute the energies at MP2/6-311++G** level using B3LYP/6-311++G** optimized geometries. Gas phase calculated results show that conformer **2B** is 2.1 kcal/mol more stable than **2A** at B3LYP/6-311++G**, which is similar to that reported by Bu and co-workers [5]. However, the energy difference decreases by ~0.6 kcal/mol in both DMSO and acetonitrile mediums. Similarly, the calculated activation barrier for the interconversion

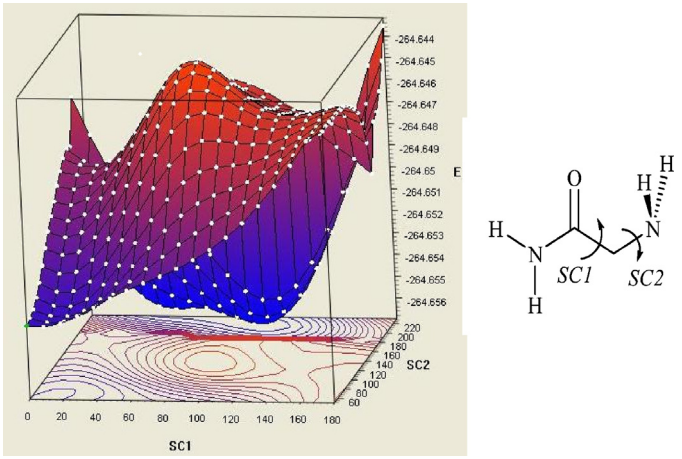

Fig. 1. B3LYP/6-311++G** calculated two dimensional potential energy surface of glycinamide in the gas phase.

of these two conformers decrease by 1.2 kcal/mol in solvents compared to the barrier calculated in the gas phase (Fig. S2, Supporting information). MP2/6-311++G** calculations also predicted similar results as observed with B3LYP/6-311++G** level of theory. DFT and *ab initio* calculations suggest that the stability of **2A** in polar solvent increases compared to the gas phase calculations. Nevertheless, **2B** is the most stable conformer in the gas and solvent phase.

To examine the influence of hydrogen bonding towards the conformational preference of glycinamide, additional calculations have been performed using both implicit and explicit solvent medium. Such hydrogen bonding interactions were examined with 6 DMSO molecules. Four DMSO molecules were engaged in H-bonding with four —N—H hydrogens of glycinamide unit and the rest 2 DMSOs interacted with the oxygen atom of the carbonyl group (Fig. 2). To achieve the intermolecular hydrogen bonding interactions between DMSO and the solute system, solvent molecules were placed in such a way to minimize the steric effects and to gain maximum H-bonding interactions. These calculations were performed using B3LYP/6-311++G** level of theory employing PCM solvation model. The single point calculations performed with MP2/6-311++G**//B3LYP/6-311++G** level of theory suggest that the conformer **2A** is energetically more stable by 5.4 kcal/mol compared to the conformer **2B** (Fig. 2). MP2 energies corrected with B3LYP zero point vibrational energy values also showed the similar preference for the stability of glycinamide conformers (Table S1, Supporting Information). These results showed the importance of hydrogen bonding between solute and solvent molecules in controlling the conformational preferences, which is different from the implicit solvent model results [5]. It is likely that DMSO might be contaminated with water in the experimental studies. Hence, we have further examined the interaction of water molecules with glycinamide analogous to DMSO in the dielectrics of DMSO medium. The calculated results with MP2/6-311++G**//B3LYP/6-311++G** level of theory suggest for the preference of conformer **2A**, similarly as with the DMSO molecules (Fig. S3, Supporting information). Further, to account the influence of dispersion forces on relative energy of glycinamide conformers, additional calculations were performed using dispersion corrected functional B3LYP-D [29]. B3LYP-D//B3LYP/6-311++G** calculated results also favour **2A** as energetically more stable conformer than conformer **2B** by 3.4 kcal/mol in DMSO medium (Table S1, Supporting Information).

To segregate the strength of interaction energies between the amine and amide —N—H hydrogens with DMSO molecules, additional calculations have been performed. B3LYP/6-311++G** optimized geometries of glycinamide interacting with 6 DMSO molecules were utilized for this purpose. To examine the interaction energy of DMSO molecules with amine hydrogens of glycinamide, other 4 DMSO molecules were detached without perturbing the geometry. In a similar fashion, interaction energy of 2 DMSO molecules with amide hydrogens was also calculated. The calculated results suggest that interaction of DMSO molecules with amide hydrogens is 4.9 and 2.0 kcal/mol stronger than the corresponding interactions with amine hydrogens for **2A** and **2B**, respectively (Fig. S4, Supporting information). The computational results though predicted the conformational preferences of glycinamide; however, an experimental verification is important at this point. We have performed ^{1}H NMR studies on the conformational equilibria of glycinamide with DMSO-d_6 and CD_3CN. Furthermore, the interaction of solvent molecules with the glycinamide conformers was explored with molecular dynamics study.

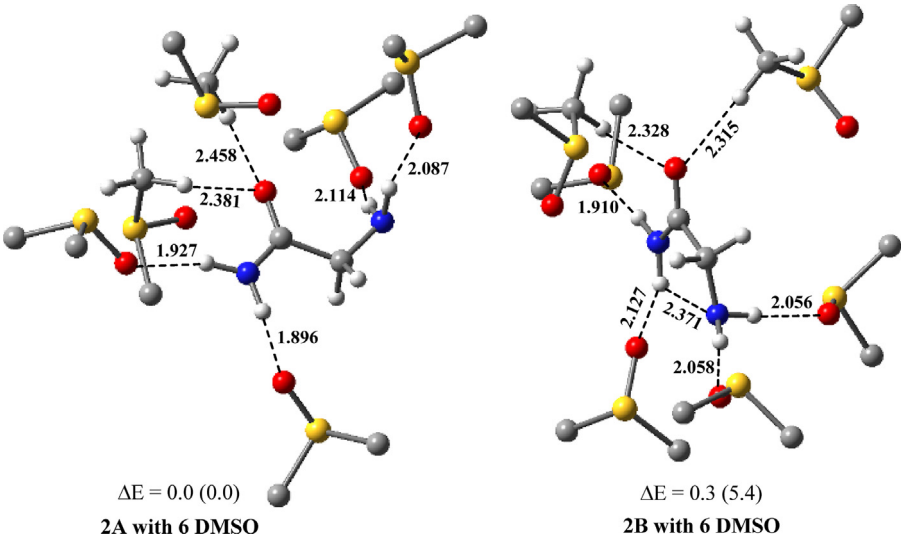

Fig. 2. B3LYP/6-311++G** optimized geometries and relative energies (kcal/mol) of glycinamide conformer **2A** and **2B** interacting with six DMSO molecules in DMSO solvent medium using PCM solvation model. MP2/6-311++G** calculated energies are given in parentheses (only selected hydrogens are shown for clarity purpose). [Gray = carbon; blue = nitrogen; red = oxygen; yellow = sulphur; white = hydrogen].

Table 1
Chemical shifts in ^{1}H NMR spectra of **1** and **2**.

Compound/solvent	H_a	H_b	CH_2	NH_2 (NH_3^+)
1/DMSO-d_6 rt	7.86	7.47	3.48	(8.12)
2/DMSO-d_6 rt	7.24	6.94	3.01	1.62
($\Delta\delta$)[a]	(0.62)	(0.53)	(0.47)	
2/DMSO-d_6 60 °C;	~7.04	~6.73	3.03	1.59
($\Delta\delta$)[b]	(0.20)	(0.21)		
2/DMSO-d_6 80 °C;	~6.8	~6.8	~3.1	–
($\Delta\delta$)[b]	(0.44)	(0.14)		
1/CD_3CN rt	~6.85	~6.35	3.61	–
($\Delta\delta$)[c]	(1.01)	(1.12)	(0.13)	
2/CD_3CN rt	~6.84	~5.85	3.15	–
($\Delta\delta$)[a]	(0.01)	(0.50)	(0.46)	
($\Delta\delta$)[c]	(0.40)	(1.09)	(0.15)	
2/CD_3CN 60 °C	~6.59	~5.75	3.18	–
($\Delta\delta$)[b]	(0.25)	(0.10)		
2/CD_3CN rt + 12 μL DMSO	~6.86	~5.91	3.14	–
2/CD_3CN rt + 22 μL DMSO	~6.89	~5.97	3.14	–
2/CD_3CN rt + 42 μL DMSO	~6.92	~6.07	3.13	–
2/CD_3CN rt + 142 μL DMSO	~7.00	~6.36	3.10	–
($\Delta\delta$)[d]	(0.16)	(0.51)		
2/C_6D_6 rt	~6.0	~4.8	2.70	–
Acetamide/$CDCl_3$ rt	~6.05	~5.82	1.94	
Formamide/D_2O rt[e]	7.3	6.9	–	–
Formamide/DMSO-d_6 rt[e]	7.43	7.16		

[a] The difference in chemical shift between protonated and non-protonated form.
[b] The difference in chemical shift at rt and at elevated temperature.
[c] The difference in chemical shift between DMSO-d_6 and CD_3CN.
[d] The difference in chemical shift between CD_3CN, and CD_3CN with the addition of DMSO-d_6.
[e] The data taken from Ref. [18].

3.1. ^{1}H NMR study

To probe the conformational behaviour of glycinamide in solution, initially, a NMR study was performed on glycinamide hydrochloride (**1**) (Scheme 1). Glycinamide is commercially available in the form of glycinamide hydrochloride. ^{1}H NMR spectrum of **1** was recorded in DMSO-d_6, which shows three well resolved signals in low magnetic field (characterized by the ratio of intensities 3:1:1) corresponding to the hydrogens of the N**H$_3$**$^+$ and two amide —CON**H$_2$** H-atoms (at 7.86 and 7.47 ppm). Assignation of the chemical shifts was based on the assignation in the ^{1}H NMR of formamide and is presented in Table 1 [30]. In the NOESY spectrum of **1**, a stronger NOE interaction is observed between the N**H$_a$**-atom and C**H$_2$**, than between the N**H$_b$**-atom and C**H$_2$**. This finding supports the conformation of **1** as shown in Fig. 1. Further, the single X-ray crystal structure of **1** was determined in our laboratory (CCDC number: CCDC 838431), which also showed the same conformation as derived by the NMR results (Scheme 1 and Fig. S5, Supporting information). These results were encouraging for further evaluation of glycinamide conformers **2** in solution. Glycinamide hydrochloride **1** was neutralized to glycinamide **2** following a procedure mentioned in Section 2.1. ^{1}H NMR spectra of **2** were taken in solvents of different polarity and at different temperatures. In addition, NOESY spectra were also recorded in DMSO-d_6 and CD_3CN at different mixing times.

In the ^{1}H NMR spectrum of **2** in DMSO-d_6, two amide N**H** signals are present at 7.24 and 6.94 ppm, whereas the amine N**H$_2$** signal appears at higher field at 1.62 ppm. As it can be seen (Table 1), deprotonation of the ammonium group in the molecule shifted signals of the amide and the methylene H-atoms in the ^{1}H NMR spectrum to the higher magnetic field for ~0.5 ppm. This shielding is in agreement with the change of the inductive effect of the substituent (from ammonium to amino group) [31].

To test if there is an intramolecular and/or intermolecular hydrogen bonding in glycinamide in DMSO-d_6, ^{1}H NMR spectra were recorded at elevated temperatures. The increase of temperature should disrupt the intermolecular hydrogen bonds (formed with the solvent molecules), whereas such an influence is expected to be milder on the intramolecular hydrogen bonds. At 60 °C, the chemical shifts of the amide N**H** signals come closer with the resonances at 7.04 and 6.73 ppm (both signals of the amide N**H** shifted for ~0.2 ppm). Further increase in temperature to 80 °C resulted in appearance of these two amide N**H** signals as one very broad singlet at 6.8 ppm, due to the cleavage of the intermolecular H-bonds with DMSO-d_6, and free rotation around —CO—N bond. Lowering the temperature gives the same appearance of the spectrum, which was observed before heating the sample. These results suggest that glycinamide presumably does not form the intramolecular H-bonding in DMSO-d_6 solution.

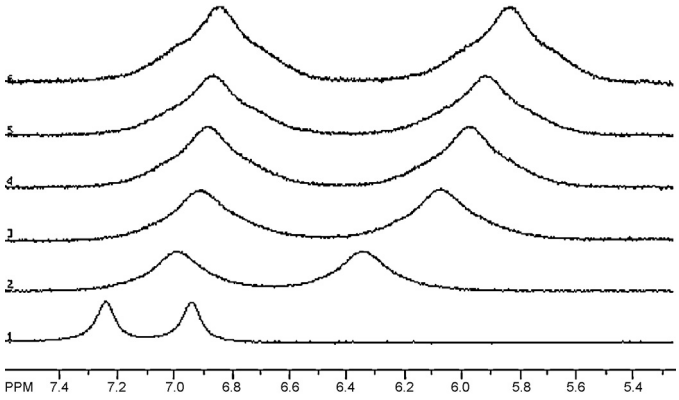

Fig. 3. Part of the ^{1}H NMR spectra of glycinamide corresponding to the amide-H atoms recorded in CD_3CN (6), CD_3CN with the increasing amounts of DMSO-d_6 (from 5–2) and DMSO-d_6 (**1**).

^{1}H NMR spectrum of glycinamide was also taken in CD_3CN, which should participate less in intermolecular hydrogen bonds with the amide-H atoms of **2** and therefore should not affect the intramolecular H-bonding, if present in the solution. The ^{1}H NMR spectrum of **2** in CD_3CN was characterized by the presence of two very broad amide N**H** singlets at δ 6.84 and 5.75 ppm, whereas C**H$_2$** appeared as a singlet at 3.19 ppm. Unfortunately, the amine N**H$_2$** signal was not seen due to the overlapping with the signal of water and/or fast exchange with the protons from water. The difference in chemical shift for the amide N**H$_a$** atom in the protonated **1** and non-protonated form **2** is negligible in CD_3CN, whereas the signal of the N**H$_b$** atom upon deprotonation shifted to the higher field for ~0.5 ppm. However, in the DMSO-d_6 both protons shifted for ~0.5 ppm. This finding suggests that H_a proton is hydrogen bonded, most probably to the amine lone pair (Scheme 1, conformer **2B**). Thus, shielding due to the deprotonation of the ammonium, and deshielding due to the hydrogen bonding gives negligible total effect in the chemical shift of the N**H$_a$** atom. Additionally, comparison of the ^{1}H NMR spectrum of acetamide with the spectrum of glycinamide in CD_3CN demonstrates that the signal of the amide N**H$_b$** atom is present at the same chemical shift, whereas glycinamide N**H$_a$** signal appears at lower magnetic field ($\Delta\delta \sim 0.8$ ppm). Consequently, it is inferred that glycinamide in CD_3CN is present in the form of conformer **2B**. To verify this assumption, ^{1}H NMR spectra were recorded also at different temperatures. Increase in the temperature resulted in line broadening in ^{1}H NMR spectrum and a larger shift of the amide N**H$_a$** signal (0.25 ppm) to the higher field than N**H$_b$** signal (0.1 ppm). This finding additionally indicates that **H$_a$** atom is hydrogen bonded. The H-bond weakens with the increase in temperature and results in a larger shift to the higher magnetic field. A similar trend as seen in CD_3CN was observed by taking spectrum of **2** in benzene-d_6, with a larger difference in the chemical shifts of the amide **H$_b$** atom (compared to DMSO).

The NMR titration performed with DMSO-d_6 also supports the existence of the intramolecular H-bond between N**H$_a$** and the

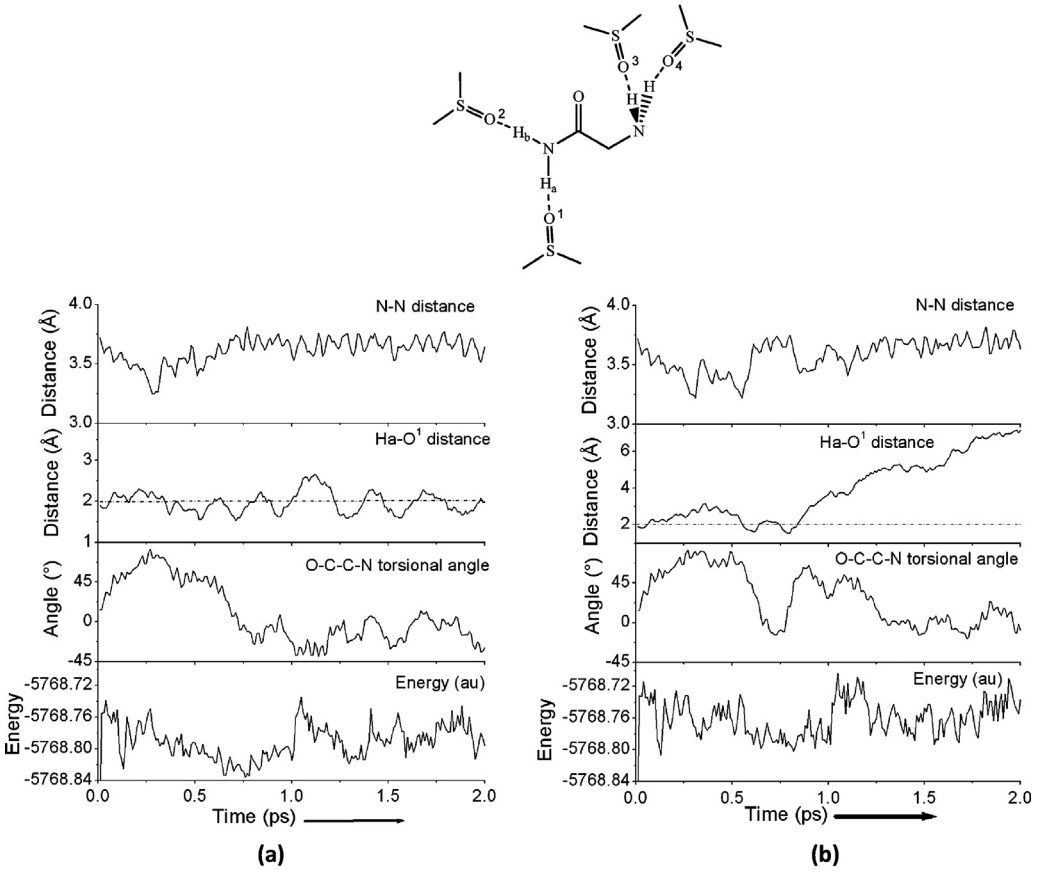

Fig. 4. LDA/PWC/DND calculated profile of variation in energy, O—C—C—N torsional angle, H_a—O^1 and N—N distance during molecular dynamics of 2 ps, (a) at 25 °C temperature and (b) at 80 °C temperature.

amine lone pair in **2**. To the solution of **2** in CD_3CN, small portions of DMSO-d_6 were added and after each addition spectra were taken. It was inferred that a small amount of DMSO-d_6 would affect first the chemical shift of the non-hydrogen bonded NH-atom, whereas a larger amount of DMSO-d_6 is necessary to break the intramolecular hydrogen bond and shifts the signal of the H-bonded atom. As expected (Fig. 3), addition of a small amount of DMSO-d_6 resulted in pronounced shifting ($\Delta\delta = 0.51$) of the N**H$_b$** and a small shifting of the N**H$_a$** signal ($\Delta\delta = 0.16$).

The ^{1}H NMR spectrum of **1** was also recorded in CD_3CN, but because of a very low solubility, the spectrum was of poor quality. However, characteristic signals corresponding to the amide-H atoms were observed at 6.85 and 6.35 ppm. By comparing ^{1}H NMR spectra of **1** in DMSO-d_6 and CD_3CN it can be seen that DMSO-d_6 deshielded the amide N**H** signals for ~1 ppm, whereas C**H$_2$** H-atoms were shielded for ~0.6 ppm. This finding also supports the conclusion that DMSO-d_6 forms intermolecular H-bondings with the amide H-atoms.

Further, the confirmation for the possible prevalence of conformer **2A** in DMSO was obtained from the NOESY spectra. In the NOESY experiment for **2** in DMSO-d_6, we have observed stronger NOE interaction between the N**H$_a$**-atom and C**H$_2$**, than between the N**H$_b$**-atom and C**H$_2$**. On the other hand, in the NOESY experiment carried out for **2** in CD_3CN and with different mixing time (0.1 s, 0.2 s, 0.3 s, 0.5 s, 0.9 s) no NOE interaction between the amide N**H**-atoms and C**H$_2$** was observed. These observations additionally support the finding obtained by DMSO-d_6 titration that glycinamide in CD_3CN most likely exists in the intramolecular hydrogen-bonded form (conformer **2B**). On the other hand, in DMSO-d_6 **1** and **2** are probably in the same conformation, or there is a free rotation around the single bond between —C═O and CH_2.

3.2. Molecular dynamics study

The conformational equilibria of glycinamide explored with the ^{1}H NMR spectra suggest that the preference of **2A** in DMSO-d_6 is due to the intermolecular hydrogen bonding at room temperature. We have performed molecular dynamics (MD) simulations to examine the dynamical nature of glycinamide **2A** in DMSO. The MD simulations will provide the effect of temperature on the rotation along O—C—C—N bond and the extent of interaction of DMSO molecules with glycinamide's amide hydrogen (H_a). The amide hydrogen H_a is crucial in governing the conformations of glycinamide as this hydrogen participates in the hydrogen bonding with the amine nitrogen in conformer **2B** (Scheme 1).

The molecular dynamic calculations were performed for glycinamide conformer **2A** interacting with DMSO molecules with local spin density approximation with the Perdew–Wang correlational (LDA/PWC) method employing DMol^3 suite program [25–27]. We used a DND double numerical basis set which is comparable to the 6-31G* basis set. Cubic box with side lengths of 15 Å were used as simulation cells. The COSMO solvation model was employed to incorporate the continuum dielectric constant environment for DMSO ($\varepsilon = 46.7$) [18,28]. The whole simulations were performed with the canonical NVT ensemble and temperature is controlled at 25 °C and 80 °C with the Nosé–Hoover chain thermostat. In each case, the simulations were initially performed for 1 ps with a time step of 2 fs (Fig. S6, Supporting information), which were further extended to 2 ps (Fig. 4). The longer simulations performed for the glycinamide conformer **2A** yields very similar information that we have received with the 1 ps. At both temperatures, the simulations were started with the conformer **2A** of glycinamide surrounded by 10 molecules of DMSO and all NH hydrogens of glycinamide are

hydrogen bonded with DMSO oxygens. The representative configuration of glycinamide surrounded by 10 DMSO molecules is given in supporting information (Fig. S7, Supporting information).

The LDA/PWC/DND simulated results show that the change in the orientation of conformer **2A** with DMSO molecules is similar up to 0.2 ps at both 25 °C and 80 °C. However, at a longer time step, *i.e.* 0.26 ps the change in the O—C—C—N torsional angle was found to be maximum (∼82°) at 25 °C. However, at 0.44 ps the O—C—C—N torsional angle reduces to 41° and then starts fluctuating between 40° and 60° till 0.64 ps. The O—C—C—N torsional angle at 25 °C appears to revert to its original situation after 0.64 ps and then further starts to rotate in opposite direction and reaches up to ∼40° and fluctuates between 13° and −40° only. The change in the O—C—C—N torsional angle with the time steps was also reflected in the distance between the glycinamide nitrogens (Fig. 4). The N···N distance of the glycinamide molecule becomes closer with the increase in O—C—C—N torsional angle. During the simulation, the intermolecular $H_a\cdots O^1$ hydrogen bond remains conserved though slight fluctuations were noticed (1.514–2.654 Å), however, from plot it is clear that most of the time this distance is below 2.0 Å (Fig. 4). The MD simulation results at 25 °C suggest that the rotation along O—C—C—N bond is possible for the conformer **2A**, however, such rotations do not perturb the intermolecular hydrogen bonding interactions between the DMSO oxygen and the amide hydrogen (H_a) as suggested in the ^{1}H NMR studies (*vide supra*).

The interaction of DMSO molecules with glycinamide **2A** simulated at 80 °C shows that the O—C—C—N torsional angle rotates to maximum (∼82°) at the time step of 0.27 ps. Further, the O—C—C—N torsional angle fluctuates between 85° and 60° up to time step of 0.54 ps, which, however reverts to the initial position (0°) and again starts to rotate after 0.72 ps. Further, at the time step of 0.9 ps, O—C—C—N torsion angle again rotates to ∼64° and then fluctuation has been observed between 28° and 53° up to 1.22 ps. The disruption in the intermolecular hydrogen bonding between **2A** and DMSO was observed as the distance varied from 1.503 Å to 3.160 Å up to time steps of 0.79 ps (Fig. 4). After 0.79 ps, the DMSO molecule interacting with H_a hydrogen atom starts to move away and another DMSO molecule approaches to H_a atom (Fig. S8, Supporting information). However, from the plot, it is clear that the $H_a\cdots O^1$ distance increases with the increase in O—C—C—N torsional angle (Fig. 4). The $H_a\cdots O^1$ distance was found to be greater than 2.0 Å in most of the simulation period, which suggests that the intermolecular hydrogen bond interrupts at the higher temperature, which is in accord to the observed ^{1}H NMR spectral results. The energy profiles obtained during the simulations at 25 °C and 80 °C show that the glycinamide conformer **2A** is energetically more stable when the intermolecular hydrogen bonding is more intact compared to that of the situation when such interactions are disrupted at elevated temperature (Fig. 4).

The molecular dynamic simulations were also carried out for glycinamide conformer **2B**, surrounded with 10 DMSO molecules, at both temperatures 25 °C and 80 °C for 1 ps. The simulation results show that at both temperatures, the intramolecular hydrogen bonding is conserved between the amide hydrogen (H_a) and amine nitrogen atom (Fig. S9, Supporting information). During the simulation period, most of the time —NH—N distance is less than 2.4 Å, which is within the intramolecular hydrogen bonding distance for —NH—N systems [32]. Further, this intramolecular hydrogen bonding restricts the rotation along O—C—C—N torsional angle of glycinamide conformer **2B**. Smaller fluctuations were observed in O—C—C—N torsional angle during the simulations at both temperatures. Interestingly, the variations in the energy of glycinamide **2A** and **2B** conformers during 1 ps simulations suggest that the conformer **2A** is more stabilized by the DMSO solvent molecules compared to the corresponding **2B** conformer during the simulations (Figs. S6 and S9, Supporting information). This is in accord with the results of quantum chemical calculations performed with DMSO molecules. Further, ^{1}HNMR results also indicate that the **2A** conformer of glycinamide should predominantly prevail in DMSO.

4. Conclusions

Our study of conformational preference of neutral glycinamide reveals interesting results to settle the debate on this topic. The computational study performed with DFT calculations by Bu et al. showed that the intramolecular hydrogen bonded glycinamide conformer **2B** is the global minimum, which contradicted the results of conformations reported by Sulzbach et al. similar to **2A** [4,5]. In the absence of experimental results the conformation study of glycinamide could not be established. We have customized in our study that both the conformers can exist in different solvent mediums. The ^{1}H NMR studies have shown that the conformer **2A** prevails in the DMSO solution, or there is a free rotation around the C—C bond. The quantum chemical calculations with hybrid solvent environment and *ab initio* molecular dynamics simulations also suggest that the conformer **2A** is more stable than that of **2B** in DMSO due to the involvement of intermolecular hydrogen bonding with solvent molecules. On the other hand, in CH_3CN conformer **2B** is likely to prevail in the solution. These results clearly suggest that the conformations of glycinamide can be altered with the nature of the solvent. The molecular dynamics simulations also supported the effect of intermolecular hydrogen bonding towards the stability of the conformer **2A**. Overall, these results showed the importance of solvent effects in controlling the conformations and can have far reaching implications in many research problems.

Supplementary data

B3LYP/6-311++G** optimized Cartesian coordinates and electronic energies of all stationary points, crystal data of compound **1** and ^{1}H NMR graphs.

Acknowledgements

This research was supported by CSIR, New Delhi, India (MSM) and the Ministry of Science, Education and Sports of the Republic of Croatia (grant no. 098-0982933-2911). MKK and AKB are thankful to UGC, New Delhi, India for awarding Fellowship. We thank the reviewers for their comments and suggestions that have helped us to improve the paper.

Appendix A. Supplementary data

Supplementary data associated with this article can be found, in the online version, at http://dx.doi.org/10.1016/j.jmgm.2013.09.007.

References

[1] A.L. Lehninger, D.L. Nelson, M.M. Cox, Principles of Biochemistry, Worth, New York, 1993.
[2] R.S. Brown, in: A. Greenberg, C.M. Breneman, J.F. Liebman (Eds.), The Amide Linkage: Structural Significance in Chemistry, Biochemistry, and Materials Science, Wiley, New York, 2000.
[3] A. Singh, S. Chakraborty, B. Ganguly, Computational study of urea and its homologue glycinamide: conformations, rotational barriers, and relative interactions with sodium chloride, Langmuir 23 (2007) 5406–5411.
[4] H.M. Sulzbach, P.v.R. Schleyer, H.F. Schaefer III, Interrelationship between conformation and theoretical chemical shifts. Case study on glycine and glycine amide, J. Am. Chem. Soc. 116 (1994) 3967–3972.
[5] P. Li, Y.X. Bu, H.Q. Ai, Conformational study of glycine amide using density functional theory, J. Phys. Chem. A 107 (2003) 6419–6428.
[6] K. Wüthrich, NMR of Proteins and Nucleic Acids, Wiley, New York, 1986.

[7] A. Singh, B. Ganguly, Probing the influence of solvent effects on the conformational behavior of 1,3-diazacyclohexane systems, J. Phys. Chem. A 111 (2007) 9884–9889.
[8] E.A. Basso, L.A. Abiko, G.F. Gauze, R.M. Pontes, Conformational analysis of *cis*-2-halocyclohexanols; solvent effects by NMR and theoretical calculations, J. Org. Chem. 76 (2011) 145–153.
[9] R.A. Nkansah, Y. Liu, O.J. Alley, J.B. Gerken, M.D. Drake, J.D. Roberts, Conformational preferences of 3-(dimethylazinoyl)propanoic acid as a function of pH and solvent; intermolecular versus intramolecular hydrogen bonding, J. Org. Chem. 74 (2009) 2344–2349.
[10] G. Lessene, B.J. Smith, R.W. Gable, J.B. Baell, Characterization of the two fundamental conformations of benzoylureas and elucidation of the factors that facilitate their conformational interchange, J. Org. Chem. 74 (2009) 6511–6525.
[11] P. Li, Y.X. Bu, H.Q. Ai, Density functional studies on conformational behaviors of glycinamide in solution, J. Phys. Chem. B 108 (2004) 1405–1413.
[12] Z.G. Huang, Y.M. Dai, L. Yu, Density functional theory and topological analysis on the hydrogen bonding interactions in N-protonated adrenaline–DMSO complexes, Struct. Chem. 21 (2010) 863–872.
[13] T. Liu, Z.-Y. Yu, Density functional theory study of the hydrogen bonding interaction of complexes of dimethyl sulfoxide with water, Asian J. Chem. 23 (2011) 1759–1763.
[14] K. Odai, S. Nishiyama, Y. Yoshida, N. Wada, ^{1}H NMR spectrum and computational study of firefly luciferin in dimethyl sulfoxide, J. Mol. Struct. (Theochem) 901 (2009) 60–65.
[15] A.D. Becke, Density-functional thermo chemistry III. The role of exact exchange, J. Chem. Phys. 98 (1993) 5648–5652.
[16] C. Lee, W. Yang, R.G. Parr, Development of the Colle–Salvetti correlation energy formula into a functional of the electron density, Phys. Rev. B 37 (1988) 785–789.
[17] W.J. Hehre, L. Radom, P.v.R. Schleyer, J.A. Pople, Ab initio Molecular Orbital Theory, Wiley, New York, 1988.
[18] J. Tomasi, M. Persico, Molecular interactions in solution: an overview of methods based on continuous distributions of the solvent, Chem. Rev. 94 (1994) 2027–2094.
[19] M. Cossi, V. Barone, R. Cammi, J. Tomasi, Ab initio study of solvated molecules: a new implementation of the polarizable continuum model, Chem. Phys. Lett. 255 (1996) 327–335.
[20] V. Barone, M. Cossi, J. Tomasi, Geometry optimization of molecular structures in solution by the polarizable continuum model, J. Comput. Chem. 19 (1998) 404–417.
[21] V. Barone, M. Cossi, J. Tomasi, A new definition of cavities for the computation of solvation free energies by the polarizable continuum model, J. Chem. Phys. 107 (1997) 3210–3221.
[22] M. Cossi, V. Barone, Analytical second derivatives of the free energy in solution by polarizable continuum models, J. Chem. Phys. 109 (1998) 6246–6254.
[23] M.J. Frisch, G.W. Trucks, H.B. Schlegel, G.E. Scuseria, M.A. Robb, J.R.J. Cheeseman, A. Montgomery Jr., T. Vreven, K.N. Kudin, J.C. Burant, J.M. Millam, S.S. Iyengar, J. Tomasi, V. Barone, B. Mennucci, M. Cossi, G. Scalmani, N. Rega, G.A. Petersson, H. Nakatsuji, M. Hada, M. Ehara, K. Toyota, R. Fukuda, J. Hasegawa, M. Ishida, T. Nakajima, Y. Honda, O. Kitao, H. Nakai, M. Klene, X. Li, J.E. Knox, H.P. Hratchian, J.B. Cross, V. Bakken, C. Adamo, J. Jaramillo, R. Gomperts, R.E. Stratmann, O. Yazyev, A.J. Austin, R. Cammi, C. Pomelli, J.W. Ochterski, P.Y. Ayala, K. Morokuma, G.A. Voth, P. Salvador, J.J. Dannenberg, V.G. Zakrzewski, S. Dapprich, A.D. Daniels, M.C. Strain, O. Farkas, D.K. Malick, A.D. Rabuck, K. Raghavachari, J.B. Foresman, J.V. Ortiz, Q. Cui, A.G. Baboul, S. Clifford, J. Cioslowski, B.B. Stefanov, G. Liu, A. Liashenko, P. Piskorz, I. Komaromi, R.L. Martin, D.J. Fox, T. Keith, M.A. Al-Laham, C.Y. Peng, A. Nanayakkara, M. Challacombe, P.M.W. Gill, B. Johnson, W. Chen, M.W. Wong, C. Gonzalez, J.A. Pople, Gaussian 03, Revision E.01, Gaussian, Inc, Wallingford, CT, 2004.
[24] M.J. Frisch, G.W. Trucks, H.B. Schlegel, G.E. Scuseria, M.A. Robb, J.R. Cheeseman, G. Scalmani, V. Barone, B. Mennucci, G.A. Petersson, H. Nakatsuji, M. Caricato, X. Li, H.P. Hratchian, A.F. Izmaylov, J. Bloino, G. Zheng, J.L. Sonnenberg, M. Hada, M. Ehara, K. Toyota, R. Fukuda, J. Hasegawa, M. Ishida, T. Nakajima, Y. Honda, O. Kitao, H. Nakai, T. Vreven, J.A. Montgomery Jr., J.E. Peralta, F. Ogliaro, M. Bearpark, J.J. Heyd, E. Brothers, K.N. Kudin, V.N. Staroverov, T. Keith, R. Kobayashi, J. Normand, K. Raghavachari, A. Rendell, J.C. Burant, S.S. Iyengar, J. Tomasi, M. Cossi, N. Rega, J.M. Millam, M. Klene, J.E. Knox, J.B. Cross, V. Bakken, C. Adamo, J. Jaramillo, R. Gomperts, R.E. Stratmann, O. Yazyev, A.J. Austin, R. Cammi, C. Pomelli, J.W. Ochterski, R.L. Martin, K. Morokuma, V.G. Zakrzewski, G.A. Voth, P. Salvador, J.J. Dannenberg, S. Dapprich, A.D. Daniels, O. Farkas, J.B. Foresman, J.V. Ortiz, J. Cioslowski, D.J. Fox, Gaussian 09, Revision B.01, Gaussian, Inc, Wallingford, CT, 2010.
[25] B. Delley, An all-electron numerical method for solving the local density functional for polyatomic molecules, J. Chem. Phys. 92 (1990) 508–517.
[26] B. Delley, Fast calculation of electrostatics in crystals and large molecules, J. Phys. Chem. 100 (1996) 6107–6110.
[27] B. Delley, From molecules to solids with the DMol^{3} approach, J. Chem. Phys. 113 (2000) 7756–7764.
[28] A. Klamt, G. Schuurmann, COSMO: a new approach to dielectric screening in solvents with explicit expressions for the screening energy and its gradient, J. Chem. Soc. Perkin Trans. 2 (1993) 799–805.
[29] S. Grimme, J. Antony, S. Ehrlich, H. Krieg, A consistent and accurate *ab initio* parameterization of density functional dispersion correction (DFT-D) for the 94 elements H–Pu, J. Chem. Phys. 132 (2010) 154104–154122.
[30] A.N. Taha, N.S. True, Experimental ^{1}H NMR and computational studies of internal rotation of solvated formamide, J. Phys. Chem. A 104 (2000) 2985–2993.
[31] E. Pretsch, P. Bühlmann, C. Affolter, Structure Determination of Organic Compounds, Springer-Verlag, Berlin, 2000.
[32] P. Fita, N. Urbańska, C. Radzewicz, J. Waluk, Ground- and excited-state tautomerization rates in porphycenes, Chem. Eur. J. 15 (2009) 4851–4856.